Mesonephric adenocarcinoma of the uterine cervix with a prominent spindle cell component

YINGYING FAN, YING HE, LIANG SUN, TIANMIN LIU and YANGMEI SHEN

Department of Pathology, West China Second Hospital, Sichuan University, Chengdu, Sichuan 610011, P.R. China

Received May 17, 2024; Accepted August 7, 2024

DOI: 10.3892/ol.2024.14641

Abstract. Mesonephric adenocarcinomas (MAs) with spindle cell components are rare malignant cervical tumours. In the present study, a retrospective analysis of these tumours was performed. Clinicopathological data were gathered from electronic surgical pathology records, and both immunohistochemistry and targeted next-generation sequencing (NGS) were performed. The present study included three postmenopausal female patients diagnosed with primary uterine cervical MA with prominent spindle cell components, aged 51-60 years. All patients underwent hysterectomy with bilateral salpingo-oophorectomy and pelvic lymph node dissection. There were no recurrences or deaths after surgery. NGS analysis identified *KRAS* mutations in 2 cases and a PIK3-catalytic subunit α (*PIK3CA*) mutation in another. Spindle cell components may indicate MAs at an advanced stage. Spindle cell components in MAs are diagnostic pitfalls, and the use of immunohistochemical panels and molecular detection cases with overlapping morphological features is recommended. While *KRAS* mutations are the most common types of mutations in MAs with spindle cell components, the present study demonstrates that *PIK3CA* mutations can also occur independently in cases without *KRAS* mutations.

Introduction

Mesonephric adenocarcinomas (MAs) are rare malignant human papillomavirus (HPV)-independent cervical tumours that arise from vestiges of the embryological female reproductive system (Wolffian/mesonephric duct) remnants located deep in the cervical wall (1,2). MAs constitute <1% of cervical adenocarcinomas (3). While these tumours can arise across a wide age range, they are rarely diagnosed in patients <30 years old (2). Clinically, this type of tumour typically manifests as abnormal vaginal bleeding or is identified as a cervical mass during a pelvic examination (4). MAs display diverse morphologic architectural patterns, including tubular, glandular, papillary, cribriform, retiform, spindle cell and solid structures (2). Morphologically, the tumour is characterized by mesonephric remnants, mesonephric hyperplasia and eosinophilic luminal secretions (5). MAs are characterized by recurrent *KRAS* mutations (3). Molecularly, 75-100% of patients with MAs exhibit *KRAS* mutations (3,6,7).

Patients with MAs have a worse prognosis compared with those with cervical squamous cell carcinoma and other types of adenocarcinomas (8,9). Spindle cell components are observable in MAs; however, they have been minimally explored in studies concerning their biological behaviour and prognosis (3). A total of 3 cases of cervical MAs that featured prominent spindle cell components are reported in the present study, and a comprehensive literature review was carried out to determine the potential associations between spindle morphology and, unique clinicopathological and molecular characteristics.

Materials and methods

Samples and clinical data. Female patients diagnosed with primary uterine cervical MA with prominent spindle cell components at West China Second University Hospital, Sichuan University (Chengdu, China) between January 2020 and December 2023 were included in the present study. All procedures performed in studies involving human participants adhered to ethical standards. The staging system used for cervical MAs with spindle cell components was the 2018 revision by the International Federation of Gynaecology and Obstetrics (FIGO) (10). The clinicopathological information of the patients, including age, clinical presentations, procedures, tumour size, follow-up information and FIGO stage, were extracted from the electronic medical records of the patients. Two gynaecological pathologists reviewed all haematoxylin and eosin (H&E) sections, and the immunohistochemical findings of the included cases. A total of 5 cases were excluded due to the lack of complete clinicopathological information or the absence of a spindle cell component. Ultimately, 3 cases were included in the present study.

Immunohistochemistry. The tissue was fixed using a 10% neutral buffered formalin solution at room temperature

Correspondence to: Professor Yangmei Shen, Department of Pathology, West China Second Hospital, Sichuan University, 1416 Chenglong Avenue, Chengdu, Sichuan 610011, P.R. China
E-mail: sym.julia@163.com

Key words: mesonephric adenocarcinomas, prognosis, next generation sequencing, KRAS, PIK3-catalytic subunit α

for 24 h. Immunohistochemical staining was performed on 4-μm-thick formalin-fixed paraffin-embedded (FFPE) tumour samples with the automated staining system Bond III (Leica Biosystems) based on the EnVision method. FFPE sections (4-μm-thick) were immersed in xylene, and 100, 95, 85 and 75% ethanol for dewaxing and hydration. Antigen retrieval was performed by heating the sections to 95˚C in citrate buffer (pH 6.0) for 20 min. For intracellular antigens or membrane proteins with an internal epitope, 0.1% Triton X-100 solution was used for permeabilization at room temperature for 10 min. The BOND polymer Refine Detection kit (cat. no. DS9800) from Leica Biosystems, using Bond III, including 3-4% hydrogen peroxide as the peroxide block, was used for 5 min at room temperature. For blocking of non-specific binding, the sections were incubated with BOND™ Primary Antibody Diluent (Leica Biosystems), which includes 1-3% BSA, at room temperature for 10 min. The sections were incubated with anti-rabbit poly-HRP IgG (<25 μg/ml; from the DS9800 kit) for 15 min at room temperature. All immunohistochemically stained tumour samples were evaluated using appropriate internal (including liver, kidney, tonsil, renal, fallopian tube and thyroid tissues) and external (including lymphocytes, mesothelial cells and normal cervical epithelial cells) controls. The chromogen used to visualize the staining was 3,3'-diaminobenzidine (included in the BOND Polymer Refine Detection kit). The following antibodies were used: Cytokeratin (CK) pan (cat. no. RAB-0050; 1:500; Fuzhou Maixin Biotechnology Development Co., Ltd.), epithelial membrane antigen (EMA; cat. no. Kit-0011; 1:100; Fuzhou Maixin Biotechnology Development Co., Ltd.), paired box 8 (PAX8; cat. no. RMA-1024; 1:200; Fuzhou Maixin Biotechnology Development Co., Ltd.), oestrogen receptor (ER; cat. no. Kit-0012; 1:100; Fuzhou Maixin Biotechnology Development Co., Ltd.), progesterone receptor (PR; cat. no. Kit-0013; 1:100; Fuzhou Maixin Biotechnology Development Co., Ltd.), p16 (cat. no. MAB-0673; 1:1,000; Fuzhou Maixin Biotechnology Development Co., Ltd.), GATA3 (cat. no. MAB-0695; 1:100; Fuzhou Maixin Biotechnology Development Co., Ltd.), CD10 (cat. no. MAB-0668; 1:400; Fuzhou Maixin Biotechnology Development Co., Ltd.), transcription termination factor 1 (TTF1; cat. no. MAB-0266; 1:100; Fuzhou Maixin Biotechnology Development Co., Ltd.), p53 (cat. no. MAB-0674; 1:1,000; Fuzhou Maixin Biotechnology Development Co., Ltd.), vimentin (Vim; cat. no. MAB-0735; 1:600; Fuzhou Maixin Biotechnology Development Co., Ltd.), hepatocyte nuclear factor-1β (HNF1β; cat. no. ZA-0129; ready-to-use; OriGene Technologies, Inc.) and Ki67 (cat. no. MAB-0672; 1:300; Fuzhou Maixin Biotechnology Development Co., Ltd.). Sections were incubated with primary antibodies at room temperature for 15 min. The immunohistochemical staining was analyzed using an Olympus BX43 light microscope (magnification, x100; Olympus Corporation).

Targeted next-generation sequencing (NGS). The genomic alteration profiling test was conducted by Precision Scientific, Inc. using targeted NGS technology. The targeted NGS panel assessed 107 genes (Table SI). DNA was extracted from unstained FFPE tumour samples from all 3 patients after selecting a region with >20% tumour cells. DNA was prepared for sequencing using the QIAamp DNA FFPE Tissue Kit (cat. no. 56404; Qiagen, Inc.) according to the manufacturer's protocol. Quality control was completed using a Qubit (Thermo Fisher Scientific, Inc.), and agarose gel electrophoresis was carried out to assess the extracted genomic DNA. Library construction and capture were performed using the KAPA HyperPlus Kit (cat. no. KK8514; Roche Sequencing), with a standard DNA starting quantity of ≥200 ng and an output library concentration of ≥0.5 ng/μl. Sequencing was conducted on the Illumina NovaSeq 6000 platform (Illumina, Inc.), using the NovaSeq 6000 S4 Reagent Kit (300 cycles; cat. no. 20028312; Illumina, Inc.), with an average sequencing depth of ≥100x for control samples and ≥500x for tumour tissue samples. The sequencing type was paired-end with a read length of 150 bp. The final library loading concentration was 300 pM, and was measured using the Qubit 3.0 Fluorometer (Thermo Fisher Scientific, Inc.). Post-sequencing, internally developed bioinformatics analysis was carried out, where the proportion of sites in the capture region with a depth >0.2x had an average depth of ≥90%, the sequence alignment rate was ≥90%, and the sequencing data Q30 were ≥80%. Variant detection included single nucleotide variations, small fragment insertions/deletions, gene copy number variations and gene fusions within the capture range with breakpoints. Data analysis was conducted using the DRAGEN Bio-IT Platform (version 3.8.4; Illumina, Inc.), and the results were interpreted using the software's variant calling pipeline (Illumina DRAGEN variant caller; https://www.illumina.com/products/by-type/informatics-products/dragen-bio-it-platform.html).

Results

Clinical features. The clinicopathological features of the patients are summarized in Table I. The present study included 3 postmenopausal female patients aged 51-60 years (mean age, 56 years) with primary uterine cervical MA with prominent spindle cell components. The 3 patients presented with different clinical symptoms, including cervical ThinPrep cytologic test results indicating abnormal (11), abdominal distension and pain, and postmenopausal vaginal bleeding. In case 1, colposcopy demonstrated a 1x0.5 cm ulcerated area on the cervix at the 11 o'clock position.

Imaging examinations indicated cervical masses in 2 cases. In case 2, a contrast-enhanced computed tomography scan demonstrated a solid-cystic mass on the left side of the pelvic cavity, measuring 7.3x6.4x5.4 cm, and unclear boundaries with the left adnexa and the posterior wall of the uterus were. Additionally, computed tomography imaging also showed a low-density uterine cervical mass in case 3, measuring 3.5x2.8x2.7 cm.

The 3 cases showed slightly elevated serum tumour markers, including serum CA125, CA19-9 and CEA. Furthermore, case 1 and 2 both had a history of surgery for pulmonary adenocarcinoma. The family histories of all patients were unremarkable.

Treatment and follow-up. All 3 patients underwent total abdominal hysterectomy and bilateral salpingo-oophorectomy (TAHBSO) with pelvic lymph node dissection (LND). Of the included patients, 2 patients were classified as FIGO

Table I. Clinicopathological features.

Parameters	Case 1	Case 2	Case 3
Age, years	51	60	57
Clinical presentation	None	Abdominal distension and pain for 1 month	Postmenopausal vaginal bleeding for 5 months
Surgical procedure	TAHBSO + LND	TAHBSO + LND + CRT	TAHBSO + LND + CT
Tumour size, cm	1	7.3	3.5
FIGO stage	IB	IIB	IIB
Gross appearance	Ulceration	Cauliflower-like mass	Cauliflower-like mass
Outcomes	DFS	DFS	DFS
Follow-up, months	9	11	16
Initial diagnosis	Synovial sarcoma	Mesenchymal tumour	Clear cell carcinoma
Imaging findings	Enlarged cervix with heterogeneous enhancement	A solid-cystic mass	A low-density mass
Serum tumour markers	CA125 and CA19-9 levels elevated	CA125, CA19-9 and CEA levels elevated	CA125 level elevated

CA, carbohydrate antigen; CEA, carcinoembryonic antigen; CT, chemotherapy; CRT, chemotherapy and radiotherapy; DFS, disease-free survival; FIGO, International Federation of Gynaecology and Obstetrics; LND, lymph node dissection; LWD, living with disease; NA, not available; TAHBSO, total abdominal hysterectomy and bilateral salpingo-oophorectomy.

stage IIB, while the remaining patient was classified as FIGO stage IB. Patients with FIGO stage IIB received postoperative adjuvant chemotherapy (CT) using carboplatin and paclitaxel for 6 cycles, while case 2 additionally underwent adjuvant radiation therapy at a dose of 6 Gy/fraction (total of 28 times).

Follow-up information was obtained for all 3 patients. The latest prognostic data showed no recurrences or deaths among the 3 patients, who were followed up for 9, 11 and 16 months.

Pathological features. On gross examination, two tumours presented as cauliflower-like masses in the cervix (Fig. 1A). A total of two biopsy specimens, one frozen and three surgical specimens were reviewed from all 3 cases.

Histologically, all surgical specimens from the 3 cases exhibited biphasic tumours characterized by the coexistence of epithelioid and spindle cell areas. There was a transition from the epithelioid areas to the spindle cell areas. In the spindle cell areas, tumour cells exhibited an invasive growth pattern, arranged in fascicular and storiform patterns (Fig. 1B). These spindle cells had small amounts of indistinct cytoplasm, oval to fusiform nuclei, non-prominent nucleoli and moderate nuclear atypia. Mitotic figures were identified. Heterologous sarcomatous components, highly heterotypic tumour cells and definite necrosis were not present.

In the adjacent area to the spindle cell areas, glandular, papillary, cribriform and back-to-back tubular structures were observed, lined by cuboidal tumour cells with moderate-to-marked nuclear atypia, mitotic figures and nuclear grooves. The cuboidal epithelioid cells formed glandular tubular structures with luminal eosinophilic hyaline secretions (Fig. 1C). Additionally, benign mesonephric remnants and hyperplasia surrounding the tumour were visible (Fig. 1D).

In the biopsy specimens of case 1, the tumour was primarily composed of spindle cells with occasional glandular components, when examined microscopically. The initial diagnosis, at the local hospital, had been synovial sarcoma. In another biopsy specimen of case 3, no spindle cell component was observed, leading to an initial diagnosis of clear cell carcinoma. Prominent spindle cell components were also observed in the frozen specimen. In the frozen sections, only diffuse spindle tumour cells were observed, with no evidence of epithelioid areas. Based on the aforementioned morphological features, the initial diagnosis of the intraoperative frozen sample was spindle cell tumour, tending towards mesenchymal tumour.

The immunohistochemistry results are shown in Table II. Immunohistochemically, tumour cells stained positive for epithelial markers, EMA and CK pan (Fig. 2A-D), PAX8 (Fig. 2E and F) and Vim (Fig. 2G and H) both in spindle cell components and in epithelioid areas. Staining for TTF1 (Fig. 2I and J) and CD10 (Fig. 2K and L) were positive in 1 case and in 2 cases, respectively. Staining for p16 (Fig. 3A and B) was focal or patchy positive in tumour cells. Tumour cells were negative or focal positive for ER (Fig. 3C and D) and PR (Fig. 3E and F) staining. Tumour cells were negative for HNF1β staining (Fig. 3G and H) in 1 case. In case 1 and 2, staining for GATA3 was positive both in spindle cell components and epithelioid areas, while in case 3, staining for GATA3 was negative in spindle cell components and positive in epithelioid areas (Fig. 3I and J). p53 was expressed at normal levels in all 3 cases (Fig. 3K and L). The range of the Ki67 proliferative index was 5-40% (Fig. 3M and N).

Molecular features. NGS was performed in all 3 cases. Microsatellite instability was not identified in any of the included cases. In case 1, only one *KRAS* mutation (p.Q61K) was identified. In case 2, one *KRAS* mutation (p.G12D) and one checkpoint kinase 2 mutation (c.909-1G>A), along with

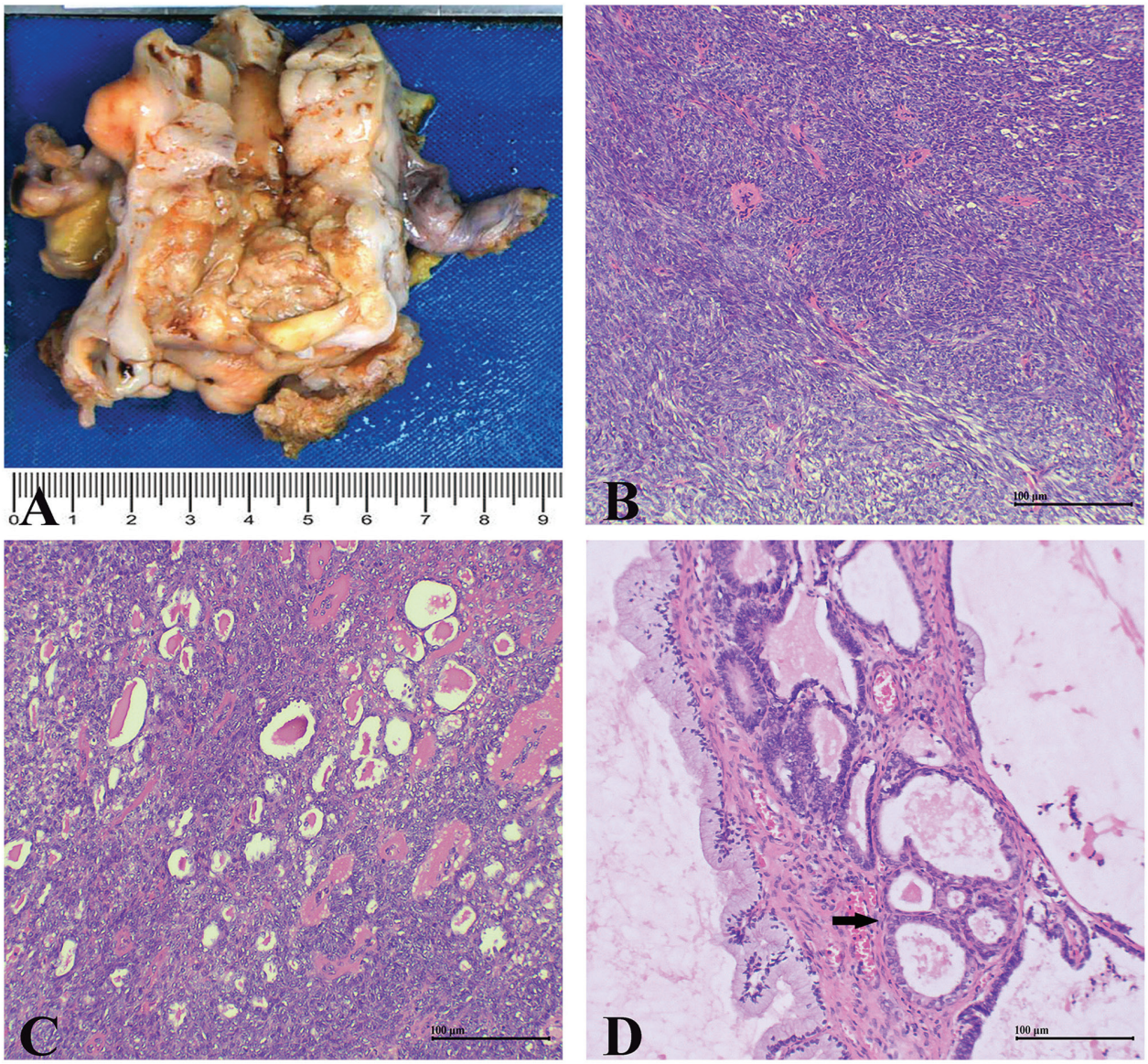

Figure 1. Gross and histological features of tumours. (A) Gross lesion presented as a cauliflower-like mass in the cervix. (B) Spindle tumour cells arranged in storiform and fascicular patterns (magnification, x100). (C) Glandular tubular structures containing eosinophilic and hyaline secretions (magnification, x100). (D) Mesonephric remnants and hyperplasia (black arrow) surrounded by epithelioid areas (magnification, x100).

amplifications of *KRAS*, *MDM4* and neurotrophic receptor tyrosine kinase 1 (*NTRK1)* were identified. A *PIK3CA* mutation (p.E726K) and amplification of *NTRK1* were identified in case 3. The histopathological and immunohistochemical findings of case 3 are shown in Fig. 4. Microscopically, the tumour consisted of two components: An epithelioid area with glandular (Fig. 4A) and papillary (Fig. 4B) patterns, and a solid spindle cell area (Fig. 4C). Immunohistochemically, both EMA (Fig. 4D) and CK pan (Fig. 4E) showed positive expression. In the epithelioid area, CD10 luminal staining was positive (Fig. 4F), and p16 staining showed patchy positive expression (Fig. 4G). PAX8 was positively expressed in both the epithelioid and spindle cell areas (Fig. 4H).

Discussion

Primary cervical MAs are rare malignant tumours, that represent only 1% of all cervical malignancies (2). Currently, cervical MAs have only been reported as case reports or small series (3,4,6,9,12,13). The largest study on cervical MAs to date is the multicentre study conducted by Pors *et al* (9), which included 30 cases. In the published literature, most MA reports did not clearly describe the presence of spindle cell components, and a few MAs with spindle cell components were diagnosed as mesonephric carcinosarcomas, previously referred to as mesonephric mixed tumours. To the best of our knowledge, only 11 cases of cervical MAs with spindle cell components have been reported, which includes the cases described in the present study (Table III).

The median age at diagnosis of cervical MAs with spindle cell components was 54 years (range, 37-76 years). The age at diagnosis was similar to that previously reported in cases of MAs without spindle cell components (52-59 years) and mesonephric carcinosarcomas (54 years) (8,9,14). The median tumour size of cervical MAs with spindle cell components was 4.5 cm (range, 1-12 cm), which was larger compared with

Table II. Immunohistochemical findings.

Parameters	Case 1		Case 2		Case 3	
	Epithelioid areas	Spindle cell areas	Epithelioid areas	Spindle cell areas	Epithelioid areas	Spindle cell areas
EMA	+	+	+	+	+	+
CK pan	+	+	NA	NA	+	+
PAX8	+	+	+	+	+	+
GATA3	+	+	+	+	+	-
CD10	-	-	+	+	+	+ (focal)
TTF1	-	-	+	+	-	-
ER	+ (focal)	+ (focal)	-	-	-	-
PR	+ (focal)	+ (focal)	-	-	-	-
p16	+ (focal)	+ (focal)	+ (patchy)	+ (patchy)	+ (patchy)	-
Vim	+	+	NA	NA	+	+
HNF1β	NA	NA	NA	NA	-	-
p53	Normal	Normal	Normal	Normal	Normal	Normal
Ki67, %	10	20	20	10	40	5

NA, not available; CK, cytokeratin; EMA, epithelial membrane antigen; PAX8, paired box 8; Vim, vimentin; TTF1, transcription termination factor; ER, oestrogen receptor; PR, progesterone receptor; HNF1β, hepatocyte nuclear factor-1β; +, positive; -, negative.

that of mesonephric carcinosarcomas (3.5 cm) (14). Among the 7 patients with MAs and spindle cell components, 5 (71%) were diagnosed at FIGO stage II-IV. A previous review reported that only 30% of patients with MAs without spindle cell components are diagnosed at FIGO stage II-IV (8). Contrary to the aforementioned review, the multicentre study by Pors *et al* (9) showed that a higher proportion of patients (60%) with MAs and without spindle cell components were diagnosed at an advanced stage (FIGO stage II-IV). Moreover, ~40% of patients with mesonephric carcinosarcomas were diagnosed at FIGO stage II-IV (14,15). These reports indicate that MAs with spindle cell components are more likely to be diagnosed at an advanced stage compared with MAs without spindle cell components and mesonephric carcinosarcomas. In the current study, spindle cell components displayed moderate nuclear atypia with readily identified mitotic figures. The advanced stage and malignant morphology suggest that spindle cell components may contribute to disease progression and aggressive biological behaviour.

Prognostic information was available for only 5 cases of MAs with spindle cell components, which includes the 3 cases presented in the present study. The mean duration of the follow-up was 16.4 months (range, 9-36 months). Only 1 patient (20%) lived with disease at FIGO stage IIIB and no death was observed. The sites of recurrence and metastasis included the abdomen, pelvis and liver (3). A previous literature review of 31 patients reported that ~30% of patients with MAs lacking spindle cell components experienced recurrence and 23% died from the disease, irrespective of the disease stage (8). The recent study by Pors *et al* (9) which included 30 cases reported that patients with MAs lacking spindle cell components had a worse prognosis, with a 5-year overall survival rate of 74% and progression-free survival rate of 60% in cervical MAs, compared with the findings of previous literature reviews. However, the composition of spindle cell components is not clearly described in the literature, which potentially makes prognostic evaluations challenging and unreliable when compared between MAs with and without these components. Patients with MAs and spindle cells components appear to have an improved prognosis compared with those patients without these components. Fregnani *et al* (16) reported that among the 35 cases of cervical adenocarcinomas, the recurrence rate was 16%, which was lower compared with that of MAs with spindle cells components. In addition, in a literature review containing 9 mesonephric carcinosarcomas, the recurrence rate was 22%, which was slightly higher compared with that of MAs with spindle cells components (8,15). Despite limited data, MAs with spindle cell components still show a poor prognosis.

In the present study, 2 of the 3 cases had a history of surgery for pulmonary adenocarcinoma. Histologically, both cases diagnosed with MAs showed glandular tubular structures with luminal eosinophilic hyaline secretions, and benign mesonephric remnants and hyperplasia. The TTF1 expression in MAs overlapped with that in pulmonary adenocarcinoma. Therefore, additional immunohistochemical markers were used to differentiate the cases. PAX8, a specific marker for differential diagnosis, was positively expressed in both cases in the present study. PAX8 primarily contributes to the organogenesis of the thyroid gland, kidney and Müllerian system. PAX8 typically shows negative expression in primary and metastatic lung cancers, and positive expression in MAs (2,17,18). The luminal staining pattern of CD10 is useful for confirming primary cervical MAs, as it is absent in pulmonary adenocarcinoma (19). Histological and immunohistochemical characteristics aided in ruling out metastatic pulmonary adenocarcinoma of the uterine cervix.

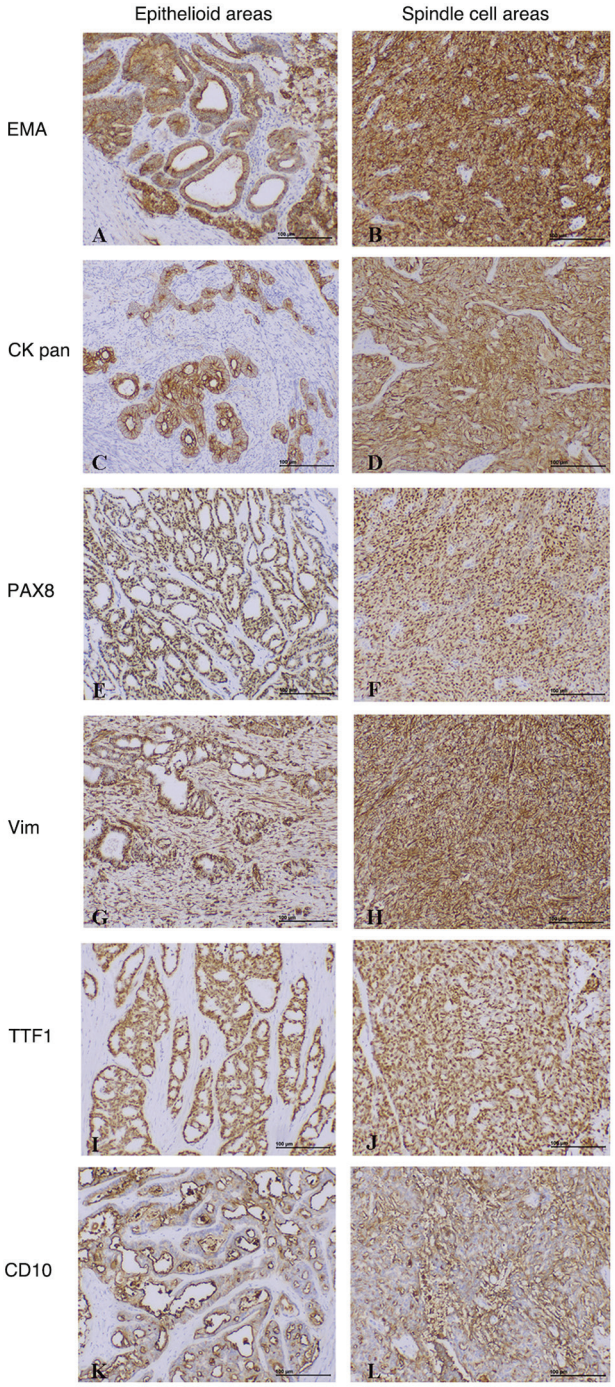

Figure 2. Representative images of immunohistochemical results from the included cases. The tumour cells showed positive expression of (A and B) EMA, (C and D) CK pan, (E and F) PAX8, (G and H) Vim and (I and J) TTF1 in both epithelioid and spindle cell areas (magnification, x100). (K) CD10 had luminal positive expression in epithelioid areas and (L) positive expression in spindle cell areas (magnification, x100). CK, cytokeratin; EMA, epithelial membrane antigen; PAX8, paired box 8; Vim, vimentin; TTF1, transcription termination factor 1.

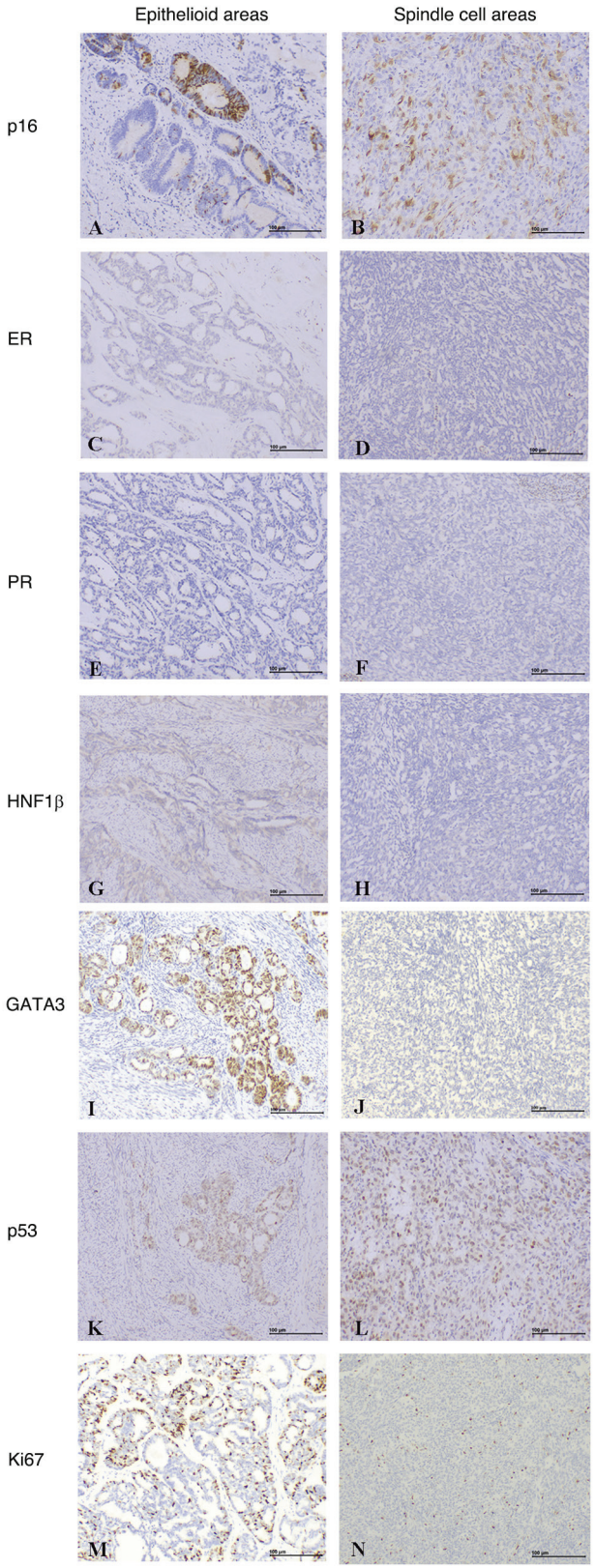

Figure 3. Representative images of immunohistochemical results from the included cases. The tumour cells showed patchy positive expression of (A and B) p16 (magnification, x100). (C and D) ER, (E and F) PR and (G and H) HNF1β were negative expression in both epithelioid and spindle cell areas (magnification, x100). (I) GATA3 had negative expression in spindle cell areas and (J) positive expression in epithelioid areas (magnification, x100). (K and L) p53 was normally expressed in tumour cells (magnification, x100). (M) Ki67 was positive in ~40% of epithelioid areas and (N) 5% of spindle cell areas (magnification, x100). ER, oestrogen receptor; PR, progesterone receptor; HNF1β, hepatocyte nuclear factor-1β.

Histologically, MAs typically exhibit a mixture of architectural patterns and overlap with other tumours (2). Spindle cell components in MAs pose diagnostic challenges and complicate accurate diagnosis. In the 2 cases reported in the present study, the initial diagnoses were initially considered to be mesenchymal tumours. Therefore, MAs should be included in the differential diagnosis when obvious spindle

Table III. Mesonephric adenocarcinomas with spindle cell components in the literature and the present cases.

First author (s), year	Case no.	Age, years	Tumour size, cm	FIGO stage	Spindle cell component, %	Outcome	Follow-up, months	*KRAS/NRAS* mutation	(Refs.)
Mirkovic *et al*, 2015	1	76	2.2	IIB	5	NA	NA	Yes	(3)
	2	47	NA	IIB	80	NA	NA	Yes	
	3	38	NA	IIIB	15	LWD	10	Yes	
	4	64	4.5	IB	60	DFS	36	Yes	
	5	67	1	NA	40	NA	NA	Yes	
	6	54	12	NA	90	NA	NA	Yes	
	7	48	NA	NA	5	NA	NA	No	
	8	37	NA	NA	30	NA	NA	No	
Present study	9	51	1	IB	80	DFS	9	Yes	-
	10	60	7.3	IIB	50	DFS	11	Yes	
	11	57	3.5	IIB	60	DFS	16	No	

FIGO, International Federation of Gynaecology and Obstetrics; DFS, disease-free survival; LWD, living with disease; NA, not available.

cell components are present morphologically, particularly in biopsy specimens. The correct diagnostic rate is only 10% in initial biopsy specimens (9). Histological and immunohistochemical features serve an important role in diagnostic work. Diagnostic clues include luminal eosinophilic hyaline secretions, nuclear grooves, mesonephric remnants, mesonephric hyperplasia, HPV independence and the absence of heterologous sarcomatous components. Recommended immunohistochemical panels include the epithelial markers EMA and/or CK pan, and PAX8, CD10, GATA3, TTF1, ER, PR, HNF1β and p16.

MAs typically exhibit positive epithelial marker expression (EMA and/or CK pan) in both epithelial and spindle cell areas, PAX8 positivity, luminal CD10 staining, negative or focal positive ER and PR, positive GATA3 and/or TTF1, negative HNF1β and non-diffuse positive p16 (18). In the present study, there were no differences in the immunohistochemical characteristics between MAs with and without spindle cell components. Among the aforementioned immunohistochemical markers, GATA3 is a highly sensitive and specific marker for MAs (20,21). In case 3, GATA3 showed negative staining in the spindle cell areas and positive staining in the adenoid areas. The staining intensity of GATA3 may decrease in the solid areas, which is consistent with previous studies (20,21). Therefore, it is noteworthy that if a spindle cell component is recognized with GATA3 expression as negative or weakly positive in the biopsy specimen, it may also be suspected of being MA. TTF1 may be useful in diagnosing cases where GATA3 is negatively expressed, due to the inverse staining pattern between GATA3 and TTF1 (21).

The overlapping morphological features of MAs with prominent spindle cell components make for a broader range of differential diagnoses. The main differential diagnoses include endocervical adenocarcinoma, clear cell carcinoma and endometrioid adenocarcinoma (2). Endocervical adenocarcinoma, often associated with HPV, exhibits mucin production or ciliation (2,4). p16 shows diffuse staining in HPV-related endocervical adenocarcinomas but shows patchy staining pattern in MAs (2,4). In cases with overlapping morphological features that are challenging to diagnose, a combination of immunohistochemical markers such as CEA, p16, GATA3 and CD10 can be used (2). Clear cell carcinoma, HPV-independent adenocarcinoma, is characterized by clear, eosinophilic and hobnailed tumour cells (22). HNF1β, a marker commonly used in the diagnosis of clear cell carcinoma, is also positively expressed in a subset of MAs (18). Squamous and mucinous differentiation can be used for the diagnosis of endometrioid adenocarcinoma (2). Immunohistochemical staining for ER and PR is usually positive in endometrioid adenocarcinoma (23).

Moreover, the most challenging differential diagnosis is that of mesonephric carcinosarcomas. Mesonephric carcinosarcomas, which are biphasic tumours, consist of distinguishable malignant epithelial and spindle cell components (6). In these two subtypes tumours, mesonephric hyperplasia and a transition from the malignant epithelioid components to the spindle cell components were observed (3,24-26), which supports both tumours originating from mesonephric duct remnants. Both MAs and mesonephric carcinosarcomas may contain a population of morphologically spindle cells, and there are no clear criteria for distinguishing between these two subtypes of tumours. The present study demonstrated that there were differences in histological and immunohistochemical features between these two subtypes tumours. In MAs, the spindle cells are typically cytologically more bland (27); however, in mesonephric carcinosarcomas, spindle cells usually show more marked atypia and heterologous sarcomatous components can also be observed (15,26). Mirkovic *et al* (27) recommended that MAs with heterologous mesenchymal elements should be diagnosed as mesonephric carcinosarcomas. At present, reported heterologous sarcomatous components in the literature have included osteosarcoma, chondrosarcoma and rhabdomyosarcoma, while the homologous component has been limited to endometrial stromal sarcoma (15). Immunohistochemically, Vim is positively expressed in 70-100% of MAs, ranging from focal positive to

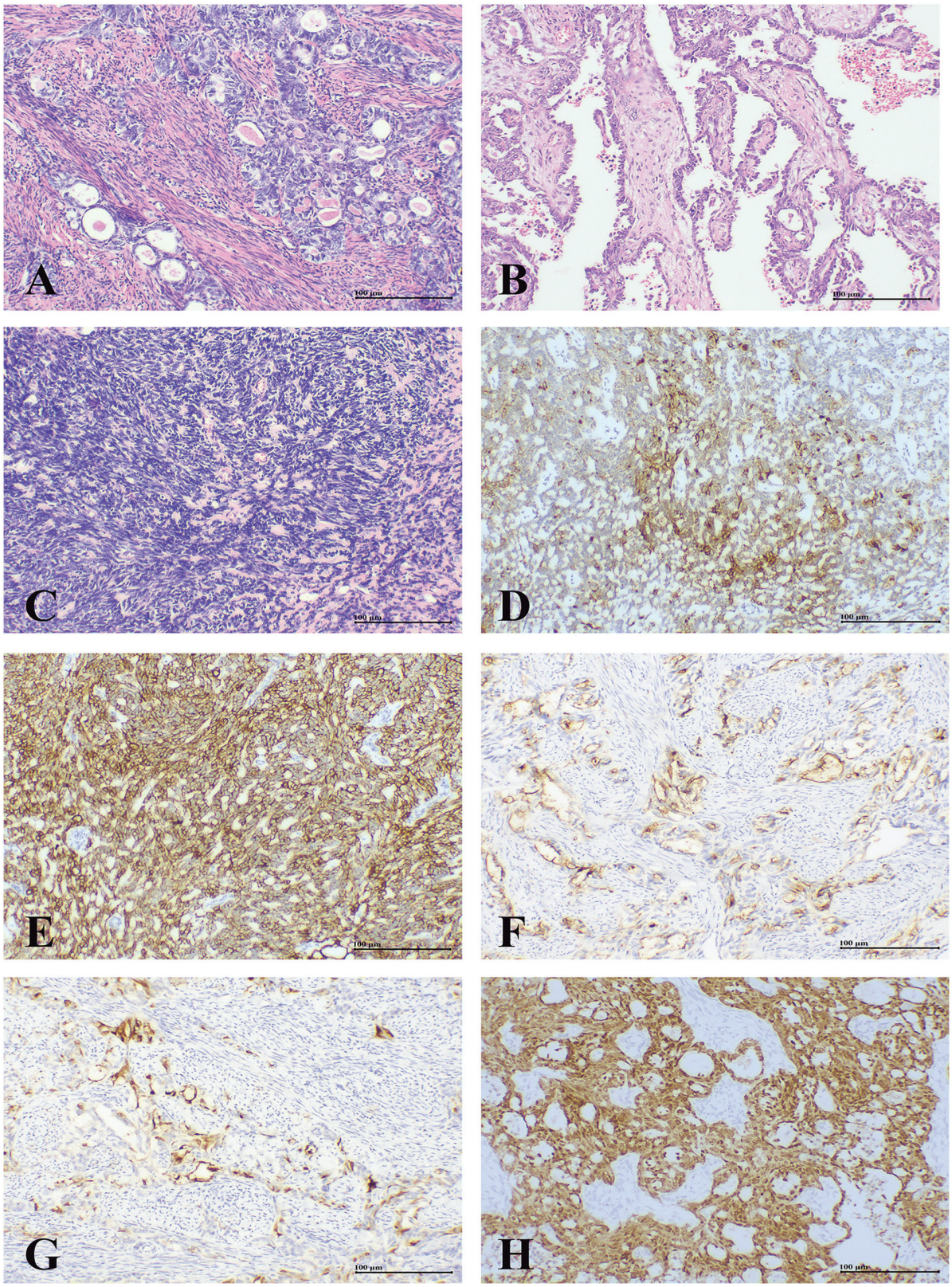

Figure 4. Pathological features of case 3. (A) Tumour cells were arranged in glands and (B) papillary patterns (magnification, x100). (C) Diffuse spindle tumour cells showed infiltrative growth in the cervical stroma. Immunohistochemical staining indicated that tumour cells in spindle cell areas were positive for (D) EMA and (E) CK pan (magnification, x100). (F) CD10 showed luminal positive expression, (G) p16 exhibited patchy positive expression and (H) PAX8 showed strong positive expression (magnification, x100). CK, cytokeratin; EMA, epithelial membrane antigen; PAX8, paired box 8.

diffuse strong positive expression (18,26). The present study showed that Vim was positively expressed in both malignant epithelioid and spindle cell areas, which showed no difference compared with mesonephric carcinosarcomas (24,25). The spindle cell components have diffuse positive expression for epithelial markers such as EMA and CK pan in MAs,

while the expression of patterns is reversed in mesonephric carcinosarcomas (15,24,25). In addition, Mirkovic *et al* (3) reported that there was no association between molecular features and spindle cell composition in MAs. Therefore, it was suggested that the spindle cell components in MAs may be part of the morphologic spectrum of the tumours, which was consistent with previous studies (27,28). Although a transition from the malignant epithelioid components to the spindle cell components was also observed in mesonephric carcinosarcomas, in contrast to MAs, the sarcomatoid spindle cell components of mesonephric carcinosarcomas may originate from the malignant epithelioid components. Similar to uterine carcinosarcoma (29), the development of sarcomatoid spindle cell components in mesonephric carcinosarcomas may be caused by epithelial-to-mesenchymal transition. In addition, the co-expression of both cytokeratin and Vim was observed in malignant epithelial areas of MAs, likely enhancing the progression of epithelial-to-mesenchymal transition (30). These may explain the lack of expression of epithelial immunohistochemical markers in spindle cell components of mesonephric carcinosarcomas and the presentation of sarcomatoid features on the histology. Therefore, epithelial immunohistochemical markers and histological features, including heterologous sarcomatous components and frankly malignant spindle cell components, are useful for distinguishing between these entities.

Consistent with previous studies (3), no specific molecular events were found to differentiate MAs with spindle cell components from those without spindle cell components. The molecular alterations of MAs without spindle cell components mainly included *KRAS/NRAS* mutations, microsatellite stability and gains of chromosome 1q (3,7). *KRAS/NRAS* mutations are the most common molecular alterations in MAs and are mutually exclusive. *KRAS* mutations are more recurrent than *NRAS* mutations, and it has been reported that the majority of patients with MAs (range, 75-100%) harboured *KRAS* mutations, which mainly affected the hotspot codons 12 and 13 (3,6,7). The mutation range of *KRAS* in cervical adenocarcinoma is 13.9-17.5%, regardless of histological type (31,32). Among the reported MAs with spindle components, including those in the present study, 72.7% exhibited *KRAS/NRAS* mutations, a rate similar to that of MAs without spindle components and markedly higher compared with that in cervical adenocarcinomas. Meanwhile, mesonephric hyperplasia lacks *KRAS/NRAS* mutations (33). *KRAS/NRAS* mutations may contribute to the development of MAs (3,6). Other molecular changes have also been reported, including chromatin remodelling of *ARID1A/B* and *SMARCA4* (3).

In the female reproductive system, *PIK3CA* mutations are more common in endometrial and other types of cervical adenocarcinomas arising from the Mullerian ducts (32,34-36). The *PIK3CA* mutation rate range is 25-32.2% in cervical adenocarcinoma, and 52% in HPV-independent cervical cancers (31,32,37). In the study by Mirkovic *et al* (3), *PIK3CA* mutations were not identified from 13 cervical MAs. Subsequently, da Silva *et al* (6) reported that 2 cervical patients with MAs harboured simultaneous *KRAS* and *PIK3CA* mutations. To the best of our knowledge, there have been no previously reported cases of *PIK3CA* mutations without *KRAS* or *NRAS* mutations in MAs or mesonephric-like carcinomas and the present study is the first to describe a case of a cervical MA with a *PIK3CA* mutation only, without *KRAS* or *NRAS* mutations. Additionally, β-catenin (*CTNNB1*) mutations are commonly found in carcinomas originating from the Mullerian ducts, and a recent study described an MA with mutations in both *CTNNB1* and *KRAS* (4). These observations suggest that there are shared molecular alterations between MAs and carcinomas that arise from the Mullerian ducts.

The present study demonstrated that MAs with spindle cell components can harbour *KRAS* and *PIK3CA* mutations independently. Activation of the mitogen-activated protein kinase (MAPK) pathway leads to abnormal activation of the RAS-MAPK pathway, promoting cellular proliferation, differentiation and survival (38). *PIK3CA* encodes the p110α catalytic subunit of the class IA PI3Ks (39). Mutations in *PIK3CA* can result in abnormally increased catalytic activity of PI3Ks, thus promoting cell carcinogenesis (39,40). According to a recent study in HPV-independent cervical cancers, aberrant activation of the PI3K-AKT pathway due to overexpression of ERBB4 and FGFR1/4 and deletion of PTEN may drive oncogenesis, affecting cell proliferation, survival and glycolysis (37). This suggests that the oncogenic drivers of these tumours may involve the RAS-MAPK and PI3K/AKT pathways, either individually or in combination. This finding provides new insights into the pathogenesis of MAs. However, the present study only included a small number of these tumour subtypes; and it remains uncertain whether this is a unique molecular alteration in MAs with spindle components. To validate the findings of the current study, NGS and whole exome sequencing on MAs without spindle components, mesonephric carcinosarcomas and sufficient MAs with spindle components are needed in future studies, which could enhance the understanding of the molecular changes in these tumours.

NTRK genes encode tropomyosin receptor kinases (Trk) (41). Fusion of *NTRK1/2/3* genes is the most common mechanism of Trk activation in various cancers (41). In malignant melanoma, the amplification of the *NTRK1* gene is associated with poor clinical outcomes (42). *NTRK1* amplification was detected in both cases of MAs with FIGO stage IIB that reported in the current study. *NTRK1* amplification may promote tumour cell proliferation in MAs leading to an advanced stage.

All 3 patients included underwent TAHBSO and pelvic LND. Of these, 2 patients received adjuvant CT with carboplatin and paclitaxel, and 1 patient also underwent adjuvant radiation therapy following primary surgery. Currently, there is no standardized treatment for this rare tumour. Treatments depend on the stage of MA, and the treatment principles are consistent with other types of cervical adenocarcinomas (12). The majority of patients with early-stage MAs underwent TAHBSO, while a small proportion of patients also received adjuvant radiotherapy and CT (8). While adjuvant CT with carboplatin and paclitaxel is commonly used as first-line treatment, its role in early-stage MAs is currently unclear (43). Similarly, the efficacy of adjuvant radiotherapy is also unclear. In the MAs lacking spindle cell components, patients receiving adjuvant therapy experienced higher recurrence and mortality rates compared with those who did not (8). Adjuvant therapy is reported to improve prognosis in patients with mesonephric carcinosarcomas that contain spindle cell components,

evidenced by lower recurrence and mortality rates compared with those not receiving therapy (15). As aforementioned, MAs with spindle cell components often present at advanced stages and have concerning recurrence rates. Therefore, it is hypothesized that adjuvant therapy is crucial for these patients as it may improve prognosis. However, larger studies are needed to clarify the clinical effectiveness of adjuvant therapy in MAs with spindle cell components.

The RAS-MAPK and PI3K-AKT pathways may be targets for therapy in MAs with spindle cell components. Common *KRAS* mutation sites include G12C, G12D and G12V (6,7). The *KRAS* G12C inhibitor adagrasib has received approval by the United States Food and Drug Administration (44). The *KRAS* G12D inhibitor has also shown promising efficacy in preclinical studies (45,46). The PI3Kα inhibitor alpelisib demonstrated therapeutic effects in cervical solid tumours (47). Additionally, in animal models, the PI3Kα inhibitor exhibited improved antitumor effects in HPV-independent cervical cancers (37). *KRAS* and *PIK3CA* mutations in MAs with prominent spindle cell components suggest that *KRAS* inhibitors and PI3K inhibitors may be used as potential targeted therapies to improve prognosis. However, KRAS and PI3Kα inhibitors have potential limitations and challenges as targeted therapies for MAs with spindle cell components. At present, there is no valid evidence of preclinical data on the efficacy of KRAS and PI3Kα inhibitors for the treatment of these rare tumours. In addition, MAs with spindle cell components are histologically biphasic tumours, and the expression of immunohistochemical markers, such as GATA3 as aforementioned, may vary between different components. Thus, it is challenging to determine the effect of the different histological components, as well as immunohistochemical expression, on the therapeutic efficacy of KRAS and PI3Kα inhibitors.

Spindle cell components in MAs have been largely overlooked in previous studies. The present study found that MAs with prominent spindle cell components were at an advanced stage and exhibited unique *PIK3CA* mutations, which distinguished them from MAs without such components. Further research is needed to gather more clinicopathological and molecular data from MAs with spindle cell components and other mesonephric tumours, to enhance the understanding of the role of spindle cell components in biological behaviour and molecular alteration. Prospective studies with larger cohorts are necessary to validate the targeted treatment with KRAS and PIK3CA inhibitors. If feasible, whole genome sequencing could provide a comprehensive genetic analysis of this rare tumour.

The present study had several limitations. Firstly, it is retrospective and spindle cell components of MAs may not be well documented in previous literature, which potentially leads to selection bias in the literature review and data collection. Secondly, the small sample size and lack of long-term follow-up limit the representativeness of the findings regarding prognosis, and molecular and clinicopathological features. Lastly, due to limited resources, the targeted NGS panel only assessed a number of gene mutations.

In conclusion, MAs exhibit morphologic diversity, with those containing spindle cell components associated with advanced stages and aggressive behaviour. Prominent spindle cell components in MAs are diagnostic pitfalls, especially in cervical biopsy specimens. Using a panel of immunohistochemical stains may aid in differential diagnosis. Despite *KRAS* being the most frequently observed molecular alteration, *PIK3CA* mutations may also be identified independently in MAs.

Acknowledgements

Not applicable.

Funding

The present study was supported by the Sichuan Science and Technology Program (grant no. 2022NSFSC0708).

Availability of data and materials

The data generated in the present study may be requested from the corresponding author. The NGS data generated in the present study may be found in the BioProject database under the accession number PRJNA1132741 or at the following URL: https://www.ncbi.nlm.nih.gov/sra/PRJNA1132741.

Authors' contributions

YF was responsible for the conceptualization, data curation and writing of the manuscript. YH and LS collected and analyzed the clinicopathologic data. TL contributed to the immunohistochemical materials preparation. YS contributed to the conceptualization, manuscript writing, review and editing, supervision and funding acquisition of the present study. YF and YS confirm the authenticity of all the raw data. All authors read and approved the final manuscript.

Ethics approval and consent to participate

The institutional ethics committee of West China Second University Hospital, Sichuan University approved this study (approval no. 2023125; Chengdu, China). Consent from patients was obtained to perform further scientific research (immunohistochemical staining and NGS) using their samples.

Patient consent for publication

Written informed consent was obtained from each patient for the publication of this article and the accompanying images.

Competing interests

The authors declare that they have no competing interests.

References

1. Sajjad Y: Development of the genital ducts and external genitalia in the early human embryo. J Obstet Gynaecol Res 36: 929-937, 2010.
2. Howitt BE and Nucci MR: Mesonephric proliferations of the female genital tract. Pathology 50: 141-150, 2018.
3. Mirkovic J, Sholl LM, Garcia E, Lindeman N, MacConaill L, Hirsch M, Dal Cin P, Gorman M, Barletta JA, Nucci MR, *et al*: Targeted genomic profiling reveals recurrent KRAS mutations and gain of chromosome 1q in mesonephric carcinomas of the female genital tract. Mod Pathol 28: 1504-1514, 2015.

4. Montalvo N, Redroban L and Galarza D. Mesonephric adenocarcinoma of the cervix: A case report with a three-year follow-up, lung metastases, and next-generation sequencing analysis. Diagn Pathol 14: 71, 2019.
5. Menon S, Kathuria K, Deodhar K and Kerkar R: Mesonephric adenocarcinoma (endometrioid type) of endocervix with diffuse mesonephric hyperplasia involving cervical wall and myometrium: An unusual case report. Indian J Pathol Microbiol 56: 51-53, 2013.
6. da Silva EM, Fix DJ, Sebastiao APM, Selenica P, Ferrando L, Kim SH, Stylianou A, Da Cruz Paula A, Pareja F, Smith ES, *et al*: Mesonephric and mesonephric-like carcinomas of the female genital tract: Molecular characterization including cases with mixed histology and matched metastases. Mod Pathol 34: 1570-1587, 2021.
7. Mirkovic J, McFarland M, Garcia E, Sholl LM, Lindeman N, MacConaill L, Dong F, Hirsch M, Nucci MR, Quick CM, *et al*: Targeted genomic profiling reveals recurrent kras mutations in mesonephric-like adenocarcinomas of the female genital tract. Am J Surg Pathol 42: 227-233, 2018.
8. Dierickx A, Goker M, Braems G, Tummers P and Van den Broecke R: Mesonephric adenocarcinoma of the cervix: Case report and literature review. Gynecol Oncol Rep 17: 7-11, 2016.
9. Pors J, Segura S, Chiu DS, Almadani N, Ren H, Fix DJ, Howitt BE, Kolin D, McCluggage WG, Mirkovic J, *et al*: Clinicopathologic characteristics of mesonephric adenocarcinomas and mesonephric-like adenocarcinomas in the gynecologic tract: A multi-institutional study. Am J Surg Pathol 45: 498-506, 2021.
10. Bhatla N, Berek JS, Fredes MC, Denny LA, Grenman S, Karunaratne K, Kehoe ST, Konishi I, Olawaiye AB, Prat J, *et al*: Revised FIGO staging for carcinoma of the cervix uteri. Int J Gynaecol Obstet 145: 129-135, 2019.
11. Klinkhamer PJ, Meerding WJ, Rosier PF and Hanselaar AG: Liquid-based cervical cytology. Cancer 99: 263-271, 2003.
12. Devarashetty S, Chennapragada SS and Mansour R: Not your typical adenocarcinoma: A case of mesonephric adenocarcinoma of the cervix with fibroblast growth factor receptor 2 (FGFR2) mutation. Cureus 14: e25098, 2022.
13. Jiang LL, Tong DM, Feng ZY and Liu KR: Mesonephric adenocarcinoma of the uterine cervix with rare lung metastases: A case report and review of the literature. World J Clin Cases 8: 1735-1744, 2020.
14. Tseng CE, Chen CH, Chen SJ and Chi CL: Tumor rupture as an initial manifestation of malignant mesonephric mixed tumor: A case report and review of the literature. Int J Clin Exp Pathol 7: 1212-1217, 2014.
15. Ribeiro B, Silva R, Dias R and Patrício V: Carcinosarcoma of the uterine cervix: A rare pathological finding originating from mesonephric remnants. BMJ Case Rep 12: e227050, 2019.
16. Fregnani JH, Soares FA, Novik PR, Lopes A and Latorre MR: Comparison of biological behavior between early-stage adenocarcinoma and squamous cell carcinoma of the uterine cervix. Eur J Obstet Gynecol Reprod Biol 136: 215-223, 2008.
17. Jeong JH, Kim NY and Pyo JS: Analysis of PAX8 immunohistochemistry in lung cancers: A meta-analysis. J Pathol Transl Med 54: 300-309, 2020.
18. Kenny SL, McBride HA, Jamison J and McCluggage WG: Mesonephric adenocarcinomas of the uterine cervix and corpus: HPV-negative neoplasms that are commonly PAX8, CA125, and HMGA2 positive and that may be immunoreactive with TTF1 and hepatocyte nuclear factor 1-β. Am J Surg Pathol 36: 799-807, 2012.
19. Kadota K, Buitrago D, Lee MC, Villena-Vargas J, Sima CS, Jones DR, Travis WD and Adusumilli PS: Tumoral CD10 expression correlates with high-grade histology and increases risk of recurrence in patients with stage I lung adenocarcinoma. Lung Cancer 89: 329-336, 2015.
20. Howitt BE, Emori MM, Drapkin R, Gaspar C, Barletta JA, Nucci MR, McCluggage WG, Oliva E and Hirsch MS: GATA3 is a sensitive and specific marker of benign and malignant mesonephric lesions in the lower female genital tract. Am J Surg Pathol 39: 1411-1419, 2015.
21. Pors J, Cheng A, Leo JM, Kinloch MA, Gilks B and Hoang L: A comparison of GATA3, TTF1, CD10, and calretinin in identifying mesonephric and mesonephric-like carcinomas of the gynecologic tract. Am J Surg Pathol 42: 1596-1606, 2018.
22. Lee Y, Bae H and Kim HS: Endocervical adenocarcinoma: Comprehensive histological review and re-classification of 123 consecutive cases according to the updated world health organization classification of female genital tumors. Anticancer Res 42: 4627-4639, 2022.
23. Masjeed NMA, Khandeparkar SGS, Joshi AR, Kulkarni MM and Pandya N: Immunohistochemical study of ER, PR, Ki67 and p53 in endometrial hyperplasias and endometrial carcinomas. J Clin Diagn Res 11: EC31-EC34, 2017.
24. Meguro S, Yasuda M, Shimizu M, Kurosaki A and Fujiwara K: Mesonephric adenocarcinoma with a sarcomatous component, a notable subtype of cervical carcinosarcoma: A case report and review of the literature. Diagn Pathol 8: 74, 2013.
25. Bague S, Rodriguez IM and Prat J: Malignant mesonephric tumors of the female genital tract: A clinicopathologic study of 9 cases. Am J Surg Pathol 28: 601-607, 2004.
26. Silver SA, Devouassoux-Shisheboran M, Mezzetti TP and Tavassoli FA: Mesonephric adenocarcinomas of the uterine cervix: A study of 11 cases with immunohistochemical findings. Am J Surg Pathol 25: 379-387, 2001.
27. Mirkovic J, Olkhov-Mitsel E, Amemiya Y, Al-Hussaini M, Nofech-Mozes S, Djordjevic B, Kupets R, Seth A and McCluggage WG: Mesonephric-like adenocarcinoma of the female genital tract: Novel observations and detailed molecular characterisation of mixed tumours and mesonephric-like carcinosarcomas. Histopathology 82: 978-990, 2023.
28. McCluggage WG: Mesonephric-like Adenocarcinoma of the female genital tract: From Morphologic observations to a well-characterized carcinoma with aggressive clinical behavior. Adv Anat Pathol 29: 208-216, 2022.
29. Matsuzaki S, Klar M, Matsuzaki S, Roman LD, Sood AK and Matsuo K: Uterine carcinosarcoma: Contemporary clinical summary, molecular updates, and future research opportunity. Gynecol Oncol 160: 586-601, 2021.
30. Kuburich NA, den Hollander P, Pietz JT and Mani SA: Vimentin and cytokeratin: Good alone, bad together. Semin Cancer Biol 86: 816-826, 2022.
31. Wright AA, Howitt BE, Myers AP, Dahlberg SE, Palescandolo E, Van Hummelen P, MacConaill LE, Shoni M, Wagle N, Jones RT, *et al*: Oncogenic mutations in cervical cancer: Genomic differences between adenocarcinomas and squamous cell carcinomas of the cervix. Cancer 119: 3776-3783, 2013.
32. Xi Q, Kage H, Ogawa M, Matsunaga A, Nishijima A, Sone K, Kawana K and Oda K: Genomic landscape of endometrial, ovarian, and cervical cancers in Japan from the database in the center for cancer genomics and advanced therapeutics. Cancers (Basel) 16: 136, 2023.
33. Mirkovic J, Schoolmeester JK, Campbell F, Miron A, Nucci MR and Howitt BE: Cervical mesonephric hyperplasia lacks KRAS/NRAS mutations. Histopathology 71: 1003-1005, 2017.
34. Cancer Genome Atlas Research Network, Kandoth C, Schultz N, Cherniack AD, Akbani R, Liu Y, Shen H, Robertson AG, Pashtan I, Shen R, *et al*: Integrated genomic characterization of endometrial carcinoma. Nature 497: 67-73, 2013.
35. Mjos S, Werner HMJ, Birkeland E, Holst F, Berg A, Halle MK, Tangen IL, Kusonmano K, Mauland KK, Oyan AM, *et al*: PIK3CA exon9 mutations associate with reduced survival, and are highly concordant between matching primary tumors and metastases in endometrial cancer. Sci Rep 7: 10240, 2017.
36. McIntyre JB, Wu JS, Craighead PS, Phan T, Köbel M, Lees-Miller SP, Ghatage P, Magliocco AM and Doll CM: PIK3CA mutational status and overall survival in patients with cervical cancer treated with radical chemoradiotherapy. Gynecol Oncol 128: 409-414, 2013.
37. Wang Y, He M, He T, Ouyang X, Shen X, Shi W, Huang S, Xiang L, Zou D, Jiang W and Yang H: Integrated genomic and transcriptomic analysis reveals the activation of PI3K signaling pathway in HPV-independent cervical cancers. Br J Cancer 130: 987-1000, 2024.
38. Olson JM and Hallahan AR: p38 MAP kinase: A convergence point in cancer therapy. Trends Mol Med 10: 125-129, 2004.
39. Samuels Y, Diaz LA Jr, Schmidt-Kittler O, Cummins JM, Delong L, Cheong I, Rago C, Huso DL, Lengauer C, Kinzler KW, *et al*: Mutant PIK3CA promotes cell growth and invasion of human cancer cells. Cancer Cell 7: 561-573, 2005.
40. Engelman JA: Targeting PI3K signalling in cancer: Opportunities, challenges and limitations. Nat Rev Cancer 9: 550-562, 2009.
41. Cocco E, Scaltriti M and Drilon A: NTRK fusion-positive cancers and TRK inhibitor therapy. Nat Rev Clin Oncol 15: 731-747, 2018.
42. Pasini L, Re A, Tebaldi T, Ricci G, Boi S, Adami V, Barbareschi M and Quattrone A: TrkA is amplified in malignant melanoma patients and induces an anti-proliferative response in cell lines. BMC Cancer 15: 777, 2015.

43. Xie C, Chen Q and Shen Y: Mesonephric adenocarcinomas in female genital tract: A case series. Medicine (Baltimore) 100: e27174, 2021.
44. Janne PA, Riely GJ, Gadgeel SM, Heist RS, Ou SI, Pacheco JM, Johnson ML, Sabari JK, Leventakos K, Yau E, *et al*: Adagrasib in non-small-cell lung cancer harboring a $KRAS^{G12C}$ mutation. N Engl J Med 387: 120-131, 2022.
45. Wang X, Allen S, Blake JF, Bowcut V, Briere DM, Calinisan A, Dahlke JR, Fell JB, Fischer JP, Gunn RJ, *et al*: Identification of MRTX1133, a noncovalent, potent, and selective $KRAS^{G12D}$ inhibitor. J Med Chem 65: 3123-3133, 2022.
46. Hallin J, Bowcut V, Calinisan A, Briere DM, Hargis L, Engstrom LD, Laguer J, Medwid J, Vanderpool D, Lifset E, *et al*: Anti-tumor efficacy of a potent and selective non-covalent $KRAS^{G12D}$ inhibitor. Nat Med 28: 2171-2182, 2022.
47. Juric D, Rodon J, Tabernero J, Janku F, Burris HA, Schellens JHM, Middleton MR, Berlin J, Schuler M, Gil-Martin M, *et al*: Phosphatidylinositol 3-kinase α-selective inhibition with alpelisib (BYL719) in PIK3CA-altered solid tumors: Results from the first-in-human study. J Clin Oncol 36: 1291-1299, 2018.